

ASSESSMENT OF AQUIFER VULNERABILITY NEAR A MAJOR DUMPSITE IN GOSHEN CITY, NASARAWA STATE, NIGERIA USING INTEGRATED GEOPHYSICAL METHODS

ABSTRACT

This study utilized geophysical methods—including Vertical Electrical Sounding (VES), 2-D Electrical Resistivity Tomography (ERT), Self-Potential (SP), and Very Low Frequency-Electromagnetic (VLF-EM) to evaluate leachate migration into aquifer systems near a major dumpsite in Goshen City, Nasarawa State. The study area, located between latitudes 8°56'8.0874"N and 8°56'8.232"N and longitudes 7°40'52.1178"E and 7°40'35.241"E, comprises basement complex and sedimentary rock formations. Fifteen VES points, three 2-D ERT profiles, ten SP profiles, and ten VLF transverses were established at the dumpsite and a control site. Geophysical data were collected using an Ohmega Allied resistivity meter and a Gem VLF receiver. Data interpretation employed tools such as WINRESIST, RES2DINV, GRAPHER, SURFER and KHFFILT. These methods identified groundwater saturation zones and contamination pathways, including fractures and faults. Results identified five to six distinct layers, including Topsoil, clayey sand, weathered/fractured, and fresh bedrocks. Leachate infiltrated zones, with low resistivity values ranging from 1.6 to 35.3 Ω .m, were identified along twelve VES points, at an average depth of 15.8 m. Negative SP anomalies are attributed to leachate electro-kinetic reactions, while high positive VLF current-density in depths of 14 m are interpreted as electrical conducting paths. The percentage (80%) of the combined VES points indicating weak to poor aquifer protective capacity, suggests that the area is unsuitable for a dumpsite establishment. The study recommends continuous monitoring and the installation of geo-synthetic clay liners at the base of the dumpsite to safeguard groundwater resources from leachate infiltration.

Keywords: Leachate, aquifer vulnerability, aquifer protective capacity, resistivity, self-potential

1.1 INTRODUCTION

The rapid population growth in Goshen City located in Karu local government area of Nasarawa State, Nigeria, driven by economic opportunities, has led to the generation of significant volumes of solid waste from domestic and industrial activities (Onicha *et al.* 2024). Improper disposal of these wastes, without adherence to engineering and environmental standards, results in leachate formation, which poses a major source of pollution to surrounding soils and groundwater (Igwegbe *et al.* 2024; Abdel *et al.* 2024). Over time, solid waste in dumpsites undergoes slow anaerobic decomposition, producing leachate alongside landfill gases, heavy metals, and various hazardous pollutants (Odoh *et al.* 2024; Sanuade *et al.* 2022). These contaminants often seep into the subsurface, potentially compromising underground aquifer systems. This study integrates geophysical methods to assess aquifer vulnerability around a major open dumpsite in Goshen City. The findings aim to inform policies and strategies for effective waste disposal and groundwater

protection. The electrical properties of leachate make geophysical techniques such as Vertical Electrical Sounding (VES), 2-D Electrical Resistivity Tomography (ERT), Self-Potential (SP), and Very Low Frequency Electromagnetic (VLF-EM) methods highly effective in mapping leachate migration pathways. In light of this, Dauda and Ali (2024) assessed the extent of leachate infiltration from waste dumpsite into groundwater resources in Gyadi-Gyadi, Kano State, Nigeria, using natural Electromagnetic (EM) field and VES methods. The study revealed an interaction between leachate and aquifer in the northern, southern, and eastern regions of the study area up to approximately 40 m depth. A group of researchers conducted a study on leachate contamination at a major dumpsite in Eket, Southern Nigeria, using VES and ERT methods (Udosen *et al.* 2024). The Dar-Zarrouk indices and electrical reflection co-efficient suggest a moderate aquifer protective capacity and potentiality in a highly heterogeneous region, suggesting the use of sanitary landfills and phyto-remediation. Another group of researchers investigated leachate infiltration and its potential influence on groundwater resources at Ojoou, Olayanju's dumpsite, southwestern Nigeria, combining geo-resistivity and natural electric field (NEF) methods (Adeniji *et al.* 2024). The study employed five dipole-dipole and five NEF measurements using Omega resistivity meters and PQWT-150 equipment, respectively. Results suggests that large portion of the study area has been contaminated by leachate.

2.1 MATERIALS AND METHODS

The Ohmega Allied resistivity metre and its accessories, hammer, electrodes/non-polarizable, measuring tape, cables, reels, Global Positioning System (GPS) and a portable GEM VLF receiver were used to obtain VES, 2-D ERT, SP and VLF-EM data. Fourteen (14) VES points with maximum current electrode spacing ($AB/2$) of 170 m using Schlumberger array configuration, two (2) 2-ERT profiles at constant electrode spacing of 5 to 120 m using Wenner array configuration, nine (9) SP profiles at constant electrode spacing of 5 to 170 m, and nine (9) VLF-EM profiles at 5 m intervals and a maximum spacing of 100 m, were established at the dumpsite. The VLF-EM data was collected using a portable GEM VLF receiver within the frequency range of 15.1 – 24.0 kHz. Data were also collected at the control centre located about 700 m away from the dumpsite by constraining each of the method along the same transverse. The data collected were interpreted using various tools, including WINRESIST, RES2DINV, GRAPHER, SURFER and KHFILT. The KHFILT tool was utilized for filtering and mapping current densities.

2.1.1 Site Location and Geology

The Goshen dumpsite and its control centre are situated between latitudes $8^{\circ}56'8.0874''N$ and $8^{\circ}56'8.232''N$ and longitudes $7^{\circ}40'52.1178''E$ and $7^{\circ}40'35.241''E$, at Aso Kadape ward in the Nyanya Gwandara general area, Karu LGA of Nasarawa State. It is underlain by the Basement Complex Rocks of Nigeria, which consists of the migmatite gneisses, the schist belts, the Older Granites suite comprising mainly different varieties of granitic rocks, including charnockites (hypersthene granites), syenites, as well as minor gabbroic and dioritic rocks, and the undeformed acid and basic dykes (Dada, 2006). These rocks have undergone polycyclic deformation, thereby causing the formation of both micro and macro structures. The general structures include joints, foliations, and faults (Dada, 2006). They generally have NNE-SSW trending gneissose foliations with few ENE-WSW and NNW-SSE trends and dip values which vary from as low as 6° to as

high as 60° in the S-E directions (Oversby, 1975; Dada, 2006; Tanko *et al.* 2015). The area is characterized by highlands and lowlands with least elevation values lower than 260 m (above sea level) in the area around the S-E, close to River Uke flow path. The highest relief point rises to heights of 410 m (asl) around S-W, which is an intrusive outcrop. The drainage pattern in the area is dendritic and this reflects a resistance to erosion by the underlying rock units. The study areas are influenced by two major climatic conditions, the rainy seasons begin in April and peaks in August through October and the dry season from February to early-mid April. The harmattan (dry and dusty wind) experienced from November - January also characterises the dry season. The mean annual rainfall is 145.66 mm per annum (Bashir, 2018).



Plate 1: Goshen Dumpsite and its control centre (Source: Google Earth)

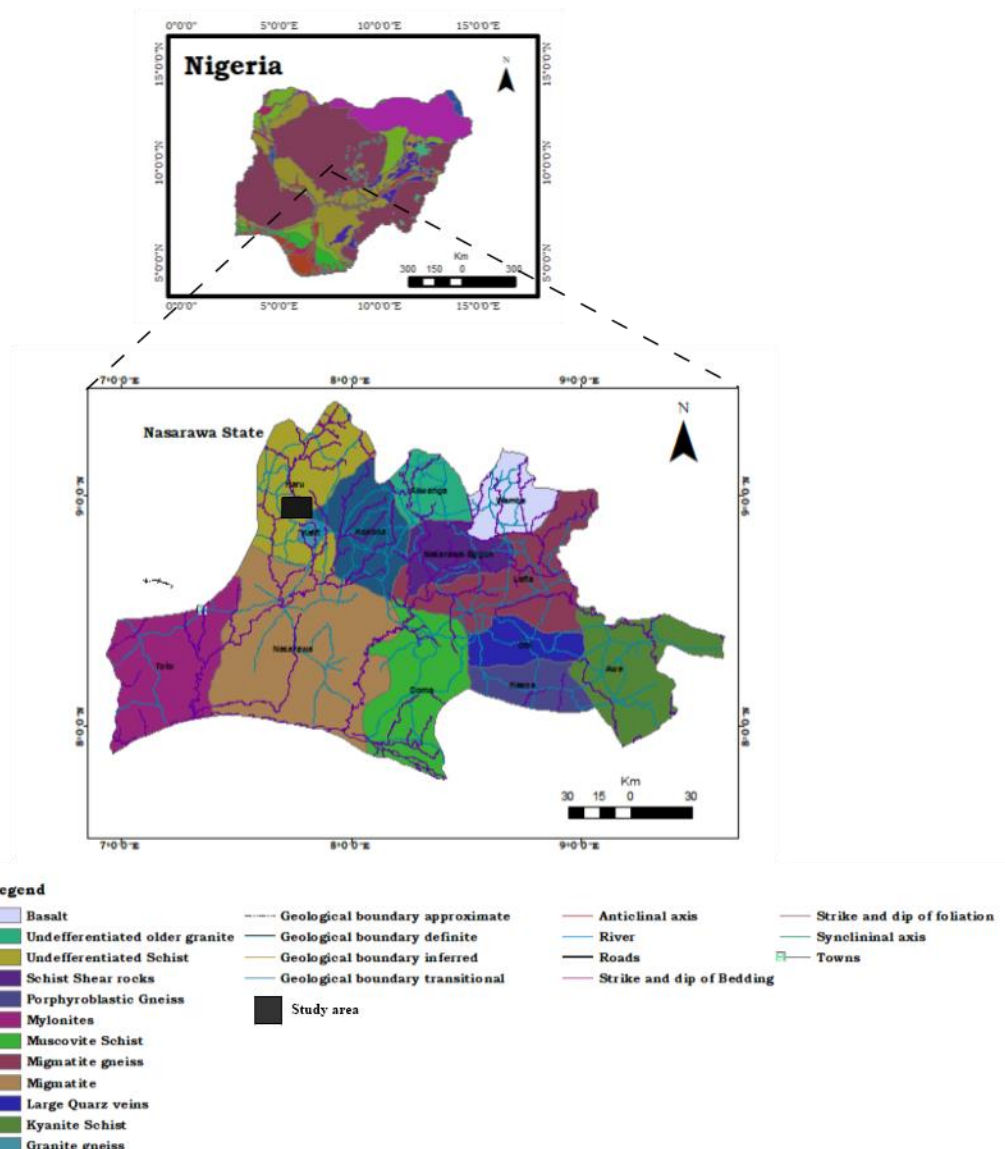


Figure 1: Geological map of the study areas (after NGSA, 2011)

3.1 RESULTS AND DISCUSSIONS

The summary of results for the fifteen (15) VES points conducted within the Goshen Dumpsite and its control centre, indicating the No. of layers, Curve Types, resistivity values ($\Omega.m$), thicknesses (m), depth (m) and delineated lithological units are presented in Table 1:

Table 1: Vertical Electrical Sounding data for VES stations 1-15 (Goshen)

VES	No. of Layer (s)	Curve Type (s)	Res. (Ω .m)	Thickness (m)	Depth (m)	Lithological Units
1	4	H	283.1	0.3	0.3	Topsoil (lateritic)
			7.0	1.9	2.2	Sandy- clay
			46651.3	175.8	178	Fresh Basement
			5631.8	-	-	Partial fresh Basement
2	5	HA	1857.9	0.9	0.9	Topsoil
			19.2	2.7	3.7	Sandy-Clay
			95.1	2.6	6.3	Weathered/Fractured basement
			18068	38.8	45	Partial fresh Basement
			30439.5	-	-	Fresh Basement
			1939.5	1.7	1.7	Topsoil
3	5	HK	35.3	2.9	4.6	Weathered layer (Saturated silt clay)
			254.9	13.5	18.1	Fractured basement
			21351.7	137.1	155.1	Partial fresh Basement
			5501.1	-	-	Fresh Basement
			2775.8	1	1	Topsoil
4	4	HK	17.6	2.7	3.6	Sandy-Clay
			1050.9	4.4	8	Partial fresh Basement
			37985.6	-	-	Fresh Basement
			3044.1	0.3	0.3	Topsoil
5	4	HA	16.6	5.2	5.5	Weathered basement
			2530.7	13.1	18.6	Partial fresh Basement
			20170.6	-	-	Fresh Basement
			96.6	1.2	1.2	Topsoil
6	5	QA	14.8	3.2	4.4	Weathered basement
			1.6	5.1	9.6	Sandy-leachate
			177.3	10.8	20.3	Weathered basement
			3278.4	-	-	Fresh Basement
			6019.8	0.8	0.8	Topsoil
7	5	H	6.4	7.7	8.5	Sandy-leachate
			77.5	15.3	23.8	Weathered basement
			3.3	99.6	123.4	Leachate
			11.3	-	-	Sand, Leachate
			217.9	1.6	1.6	Topsoil (Lateritic)
8	5	HA	3.9	2	3.7	Sandy-Leachate
			30.3	2	5.7	Weathered basement
			9178.4	76	81.7	Fresh Basement
			5901.5	-	-	Partial fresh Basement

9	4	HK	128.5	1	1	Topsoil
			28.3	4.4	5.4	Clayey-sand
			26784.7	159.4	164.8	Fresh Basement
			3950.9	-	-	Partial fresh Basement
10		HA	91.2	1.3	1.3	Topsoil
			20.8	2.3	3.6	Saturated sandy soil
			389.2	2.9	6.5	Fractured basement
			44739.6	-	-	Fresh Basement
11		KH	223.6	1.4	1.4	Topsoil
			295.9	2.5	3.9	Weathered/Fractured layer
			140.8	6.2	10.1	Weathered basement
			614428	-	-	Fresh Basement
12		HK	371.8	0.5	0.5	Topsoil
			12.4	1.3	1.8	Sandy clay
			366	1.6	3.4	Fractured basement
			100000	-	-	Fresh Basement
13		KH	141.8	0.8	0.8	Topsoil
			517.4	1.9	2.7	Weathered/Fractured basement
			82.1	5.2	7.8	Weathered
			81,656.2	-	-	Fresh Basement
14		HK	117	1.5	1.5	Topsoil
			13.8	1.9	3.5	Sandy-clay
			1585.9	5.1	8.5	Fresh basement
			37615	-	-	Partial fresh Basement
15	3	A	59.3	3	3	Topsoil
			42612.2	20	23	Partial fresh Basement
			100000	-	-	Fresh Basement

3.1.1 Estimated Aquifer Parameters of the surveyed area (Goshen)

The primary aquifer parameters (resistivity and thickness) are determined from Table 1 and used to estimate the geo-hydraulic parameters. The summary of the Dar-Zarrouk parameters estimated for the weathered aquifers showing the VES points, resistivity values ρ ($\Omega.m$), Aquifer thicknesses h (m), Electrical conductivity σ ($\Omega.m^{-1}$), Longitudinal Conductance S (mhos), Transverse Resistance T_R ($\Omega.m^{-2}$), Hydraulic conductivity K (m/day), Transmissivity T (m^2/day), Quantity of water and porosity ϕ (%) are presented in Tables 2 and 3:

Table 2: The summary of Dar-Zarrouk parameters and electrical conductivity K (m/day) estimated for the weathered aquifers in the study area (Goshen)

VES	ρ ($\Omega.m$)	Thickness (h/m)	$\sigma = 1/\rho$ ($\Omega.m^{-1}$)	$S = \sigma h$ (mhos)	$T_R = h\rho$ ($\Omega.m^{-2}$)	K (m/day)
-----	--------------------------	--------------------	--	--------------------------	--------------------------------------	----------------

1	7.0	1.9	0.1429	0.2714	13.3	62.908
2	95.1	2.6	0.0105	0.0273	247.1	5.517
3	254.9	13.5	0.0039	0.0529	3441.1	2.199
4	17.6	2.7	0.0568	0.1534	47.52	26.618
5	16.6	5.2	0.0602	0.3132	86.32	28.111
6	177.3	10.8	0.0056	0.0609	1914.84	3.086
7	3.3	99.6	0.3030	30.1818	328.68	126.870
8	30.3	2.0	0.0330	0.0660	60.6	16.036
9	28.3	4.4	0.0353	0.1555	124.52	17.090
10	389.2	2.9	0.0026	0.0075	1128.68	1.482
11	140.8	6.2	0.0071	0.0440	872.96	3.826
12	366	1.6	0.0027	0.0044	585.6	1.569
13	82.1	5.2	0.0120	0.0630	426.92	6.328
14	13.8	1.9	0.0724	0.1380	26.22	33.398
15	42612	20	2.4E-05	0.0004	852244	0.0185

Table 3: The summary of aquifer transmissivity (T), quantity of water Q and porosity ϕ (%) estimated for the weathered aquifers in the study area (Goshen)

VES	T = kh (m ² /day)	Quantity Q = (k σ)	Porosity ϕ (%)
1	119.525	8.9868	44.14
2	14.35	0.06	33.19
3	29.6918	0.0086	29.05
4	71.870	1.5124	40.27
5	146.179	1.6934	40.51
6	33.3271	0.0174	30.57
7	12636.0	38.444	47.29
8	32.0725	0.5293	37.99
9	75.20	0.604	38.27
10	4.2978	0.0038	27.27
11	23.722	0.0272	31.54
12	2.511	0.0043	27.53
13	32.907	0.077	33.80
14	63.456	2.420	41.29
15	0.3711	4.4E-07	7.56

3.1.2 Results of computer modeled curve for fifteen (15) VES points (Goshen)

The results of the computer modeled curves for the fifteen (15) VES points conducted within Goshen dumpsite and its control centre are shown in Figures 2 to 16:

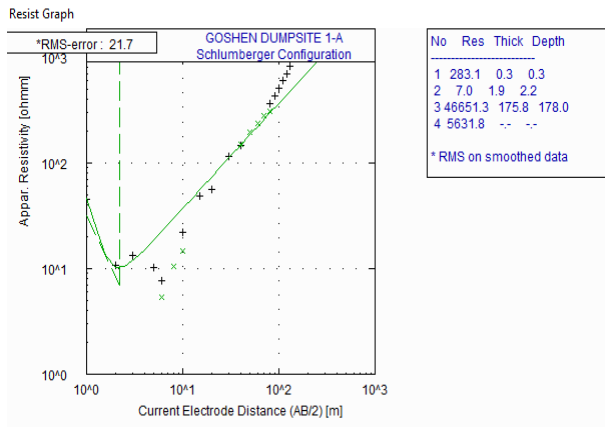


Figure 2: Results of computer modeled curve for VES 1

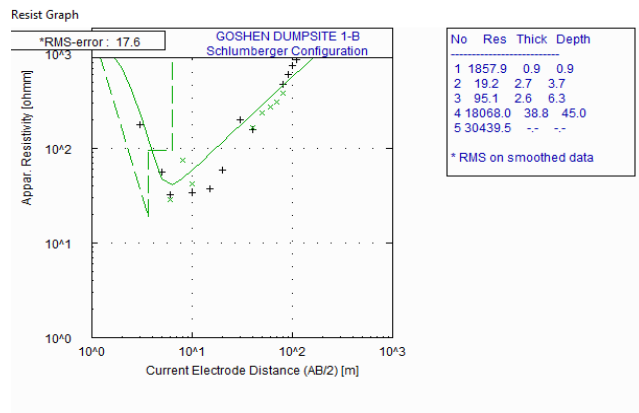


Figure 3: Results of computer modeled curve for VES 2

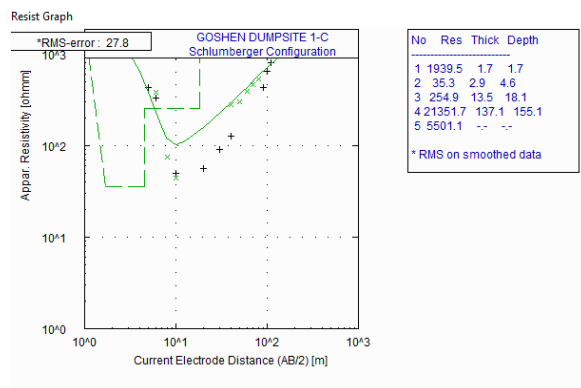


Figure 4: Results of computer modeled curve for VES 3

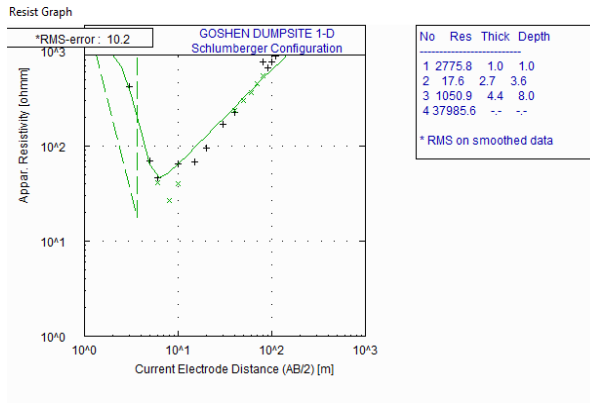


Figure 5: Results of computer modeled curve for VES 4

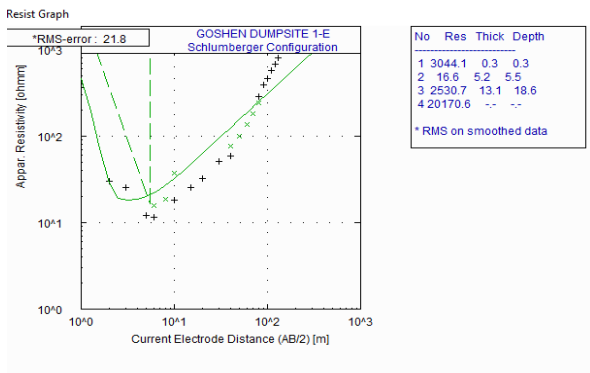


Figure 6: Results of computer modeled curve for VES 5

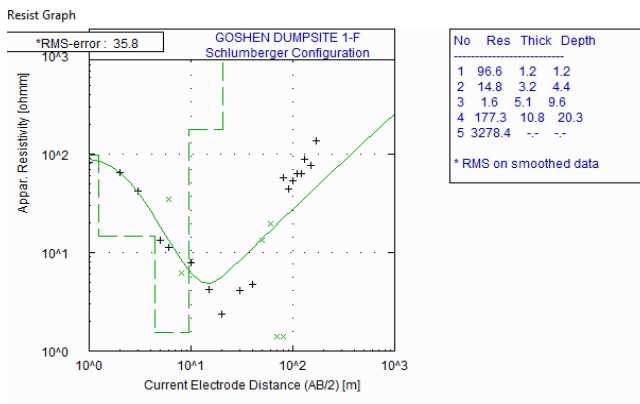


Figure 7: Results of computer modeled curve for VES 6

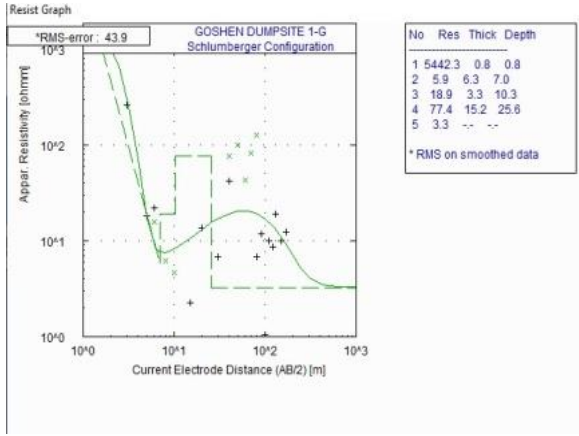


Figure 8: Results of computer modeled curve for VES 7

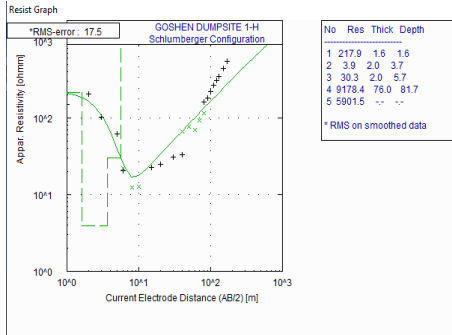


Figure 9: Results of computer modeled curve for VES 8

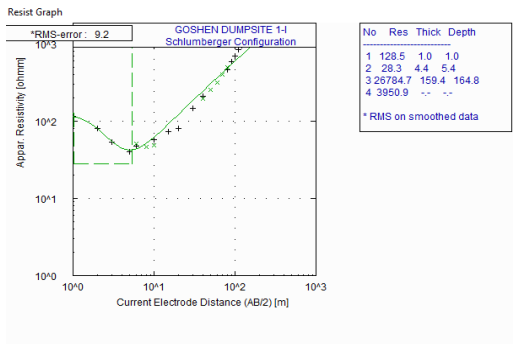


Figure 10: Results of computer modeled curve for VES 9

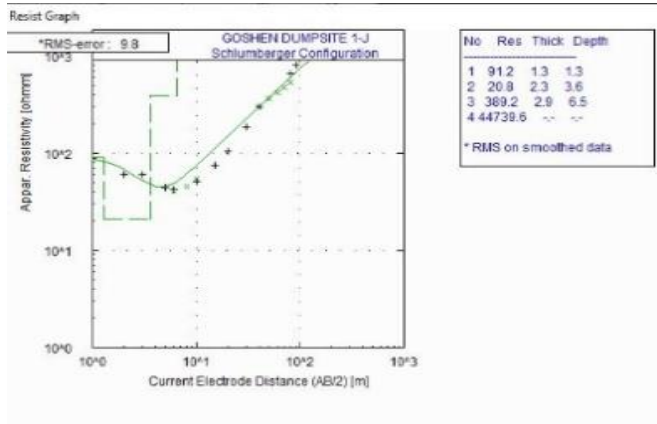


Figure 11: Results of computer modeled curve for VES 10

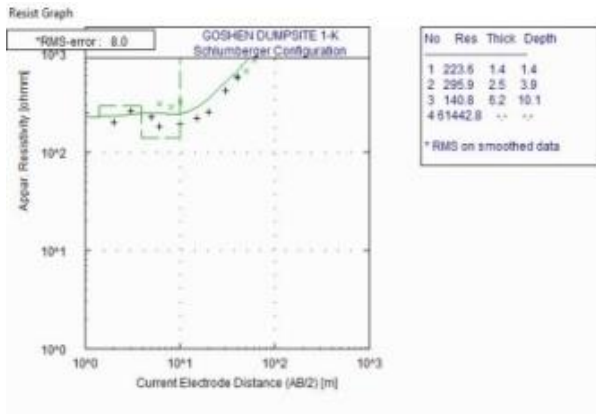


Figure 12: Results of computer modeled curve for VES 11

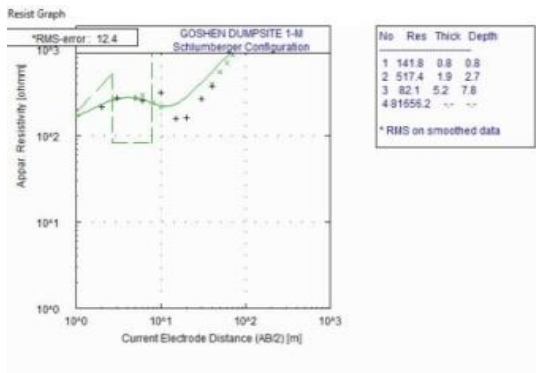


Figure 13: Results of computer modeled curve for VES 12

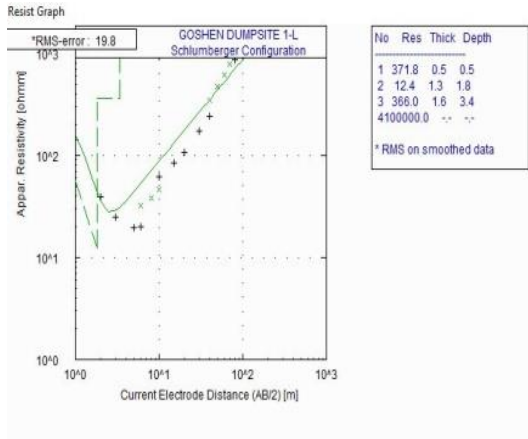


Figure 14: Results of computer modeled curve for VES 13

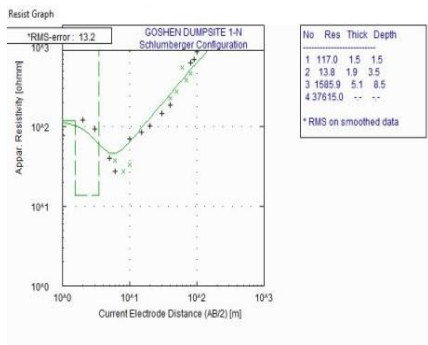


Figure 15: Results of computer modeled curve for VES 14

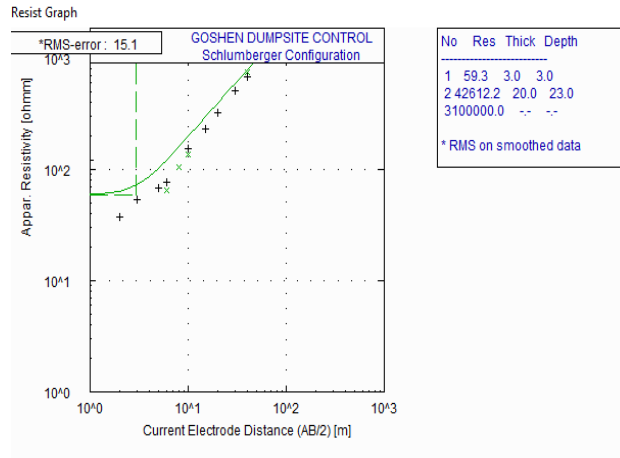


Figure 16: Results of computer modeled curve for VES 15 (Control)

3.1.3 Correlation of Borehole log with VES

The correlation of borehole lithological logs BH (D) and BH (C) (Peter *et al.* 2016) with resistivity sounding (VES) results for VES 1-6 and for VES 7 – 15 for the study area are shown in Figures 17 and 18:

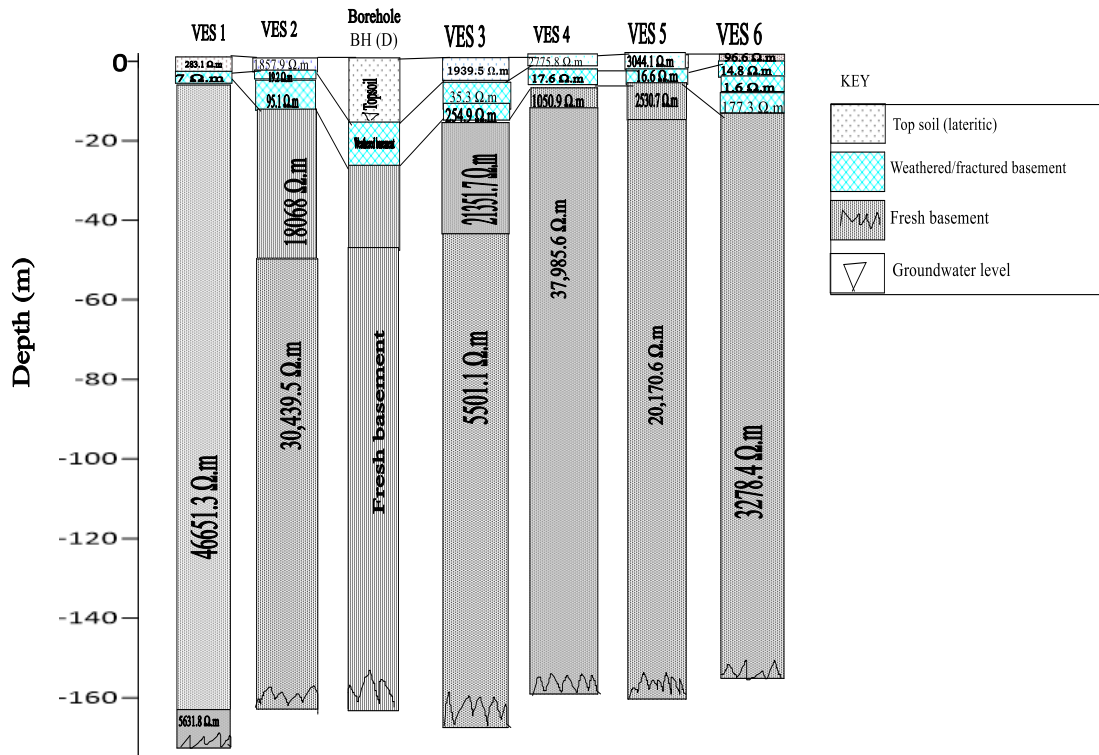


Figure 17: Correlation of resistivity sounding (VES) results with borehole lithological logs in the study area

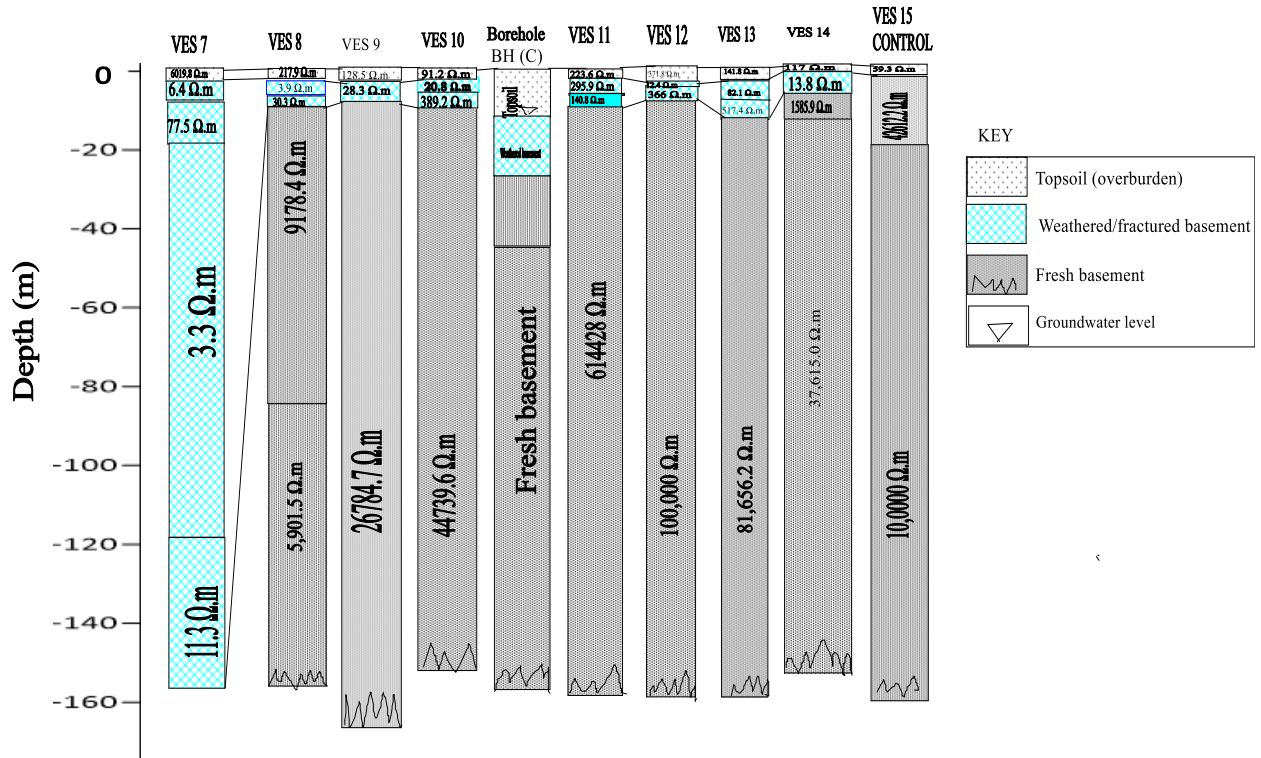


Figure 18: Correlation of resistivity sounding (VES) results with borehole lithological logs in the study area

3.1.4 Discussion

The measured apparent resistivity curves and results of the 1-D inversion that correlate well with the measured values are displayed in the corresponding resistivity-depth profiles in Figures 17 and 18. The VES data revealed four to five discrete geo-electric layers, such as Topsoil consisting of lateritic soil; second layer - interpreted as clayey sand; third layer - inferred as weathered/fractured; the fourth and fifth layers - interpreted as fresh bedrock. The Curve Types identified from the model include: HA (26.7 %), HK (26.7 %), H (13.3 %), KH (13.3 %) QA (6.7 %), while the A (6.7 %) type curve was identified at the Control Centre.

3.1.5 The Topsoil

Resistivity values for Topsoil ranges from (96 to 1857.9 $\Omega.m$) with corresponding depths ranging from (0.3 to 3 m) and thicknesses (0.3 to 3 m). This is suggestive of three zones: the belt of the soil water at the top, the intermediate vadose zone, and the capillary fringe at the bottom which acts as the passage for the flow of surface water to the fractured layer known as the zone of aeration. This layer correlated with the borehole logs.

3.1.6 The Second layer

The resistivity values of the second layer ranges from (3.9 to 35 $\Omega.m$) with corresponding depths of (2.2 to 8.5 m) and thicknesses ranging from (1.9 to 7.7 m). This layer is mostly composed of weathered to fractured basement, clay, leachate and consolidated sandstones capable of hosting

groundwater resources. The varying levels of compaction in the clayed sand may account for the contrasting resistivity values in this layer This layer correlated with the borehole logs.

3.1.7 The third layer

The resistivity values of the third layer ranges from (1.6 to 2530.7 Ω .m) with corresponding depths ranging from (3.4 to 178 m) and thicknesses (1.6 to 159.4 m). This is likely composed of clay, weathered/fractured basement to fresh basement. The increase in resistivity values in basement rocks is a function of lower fracture density or lower levels of weathering as seen in the boundary between layers 3 and 4, close to the fresh basement, with the resistivity values of the fourth layer ranging from (3,950.9 to 26784.7 Ω .m), with corresponding depths ranging from (20.3 to 155.1 m) and thicknesses (10.8 to 137.1 m). The resistivity values tend to increase towards the boundary between layers 3 and 4 attributed to the increase in grain size. This layer also correlated with the borehole logs.

3.1.8 The conductive layers

Conductive layers with resistivity values lesser than (1.6 to 35.3 Ω .m, average depths \geq 15.8 m) were delineated as leachate infiltrated and soil-contaminated zones. This spread along transverses 1, 2, 3, 4, 5, 6, 7, 8, 9, 10, 12 and 14 to a maximum depth of about 123.4 m and at an average depth of 15.8 m.

3.1.9 Estimated Aquifer Protective Capacity (APC) for Goshen study area

The calculated Longitudinal Conductance S (mhos) (Tables 3 and 4) revealed that the aquifer protective capacity of the study area is rated as poor to excellent with VES 7 (30.18 S) representing (6.7%) rated as excellent; VES 1 (0.27 S) and VES 5 (0.31 S) representing (13.3 %) rated as moderate, VES points, VES 4 (0.153 S), VES 9 (0.155 S), VES 14 (0.14 S) representing (20 %) rated as weak, while, VES 8 (0.066 S), VES 6 (0.061 S), VES 3 (0.053 S), VES 11 (0.044 S), VES 2 (0.027 S), VES 10 (0.0075 S), VES 13 (0.0063 S), VES 12 (0.0044 S), VES 15 (0.00046 S), representing 60 % of the sounding points - rated as poor. The combined rating of VES points indicating weak to poor protective capacity (80 %), suggests that the study area is not suitable for the establishment of a dumpsite, as there is no sufficient impervious clay seal to protect groundwater resources from leachate infiltration.

3.2 Results of the Self-Potential (SP) survey conducted in the study area

The results of the ten (10) SP profiles conducted in the study area are shown in Table 4:

Table 4: Summerised results from Self-Potential (SP) survey in the study area

Distance X (m)	SP (mV) 1	SP (mV) 2	SP (mV) 3	SP (mV) 4	SP (mV) 5	SP (mV) 6	SP (mV) 7	SP (mV) 8	SP (mV) 9	SP (mV) 10 (Control)
0	-99	-44.3	8.3	-13.5	-63.3	151	-50	-48	-35	92
5	-27	-80	-28	-14.7	-91.2	143	-133	-24	81	154
10	1.8	-26	-5.3	-43.4	-69.3	127	-34	11.4	2.7	144

15	39.5	-65.8	-32	-11.1	-143	67	-33	-76	111	84
20	6.31	-29.7	30	-14.1	-101	33	-59	-8.8	174	150
25	11	-113	49	-14	-49.4	14	-23	-34	86	33
30	-22	-92	92	-10.8	-70.3	23	-39	-39	-10	163
35	53.1	-47.3	93	72.1	-71.5	-8.3	-74	-33	18	108
40	39.6	-30.1	49	56.7	-75.4	37	-89	-59	-9	137
45	8.59	57.6	48	37.7	-86.9	138	-578	-35	22	122
50	80.1	8.14	97	88.7	-78.5	72	-231	-38	-32	136
55	8.65	-16.8	50	102.	-84.2	71	-78	-91	32	123
60	18.5	25.6	9.6	70.5	-77.5	133	-146	-59	-23	137
65	15	24.18	40	105.5	-95.7	28	0.7	-5.4	-26	171
70	9.59	-78.9	8.8	99.6	-90.8	57	-105	-11	4.6	208
75	56.2	26.53	100	30.63	-128	41	-57	-42	52	247
80	-66	18.13	55	73.98	-49.6	57	-39	3.34	-47	170
85	-55	11.98	4.4	226.2	-47.8	9.7	-69	15	-21	239
90	-59	10.75	32	63.94	-68.9	59	-85	-7	45	262
95	9.37	28.38	72	55.74	-38.3	140	-26	80.3	18	165
100	-28	43.85	41	-0.44	102.4	124	-113	49.6	-41	227
105	52.3	58.2	34	72.54	-93.5	83	-11	28.9	15	203
110	73	40.37	84	130.1	-32.2	144	-29	27.7	-85	206
115	-3.8	-12.8	58	159.3	-56.4	119	-41	27.2	30	239
120	-4	-4.14	-35	51.64	-44.7	152	-105	3.98	2.4	206
125	41.8	11.27	-5.3	69.4	-43.7	-1.2	-121	28.6	6.9	159
130	-5.1	-1.46	23	94.88	-67.8	109	-96	-69	-6	211
135	14.1	26.64	76	63.32	-88.3	154	-67	-114	-24	143
140	-14	13.42	17	95.91	-34	144	-65	-18	-1	202
145	-86	18.54	-3.3	97.55	-96.3	113	-42	-109	27	181

150	-18	50.62	-2.4	101.2	-77.5	29	26	-109	66	225
155	29.7	-24.8	-	138.3	-34.8	-	-	-102	9.6	171
160	-	-	-	-	-	-	-	-87	-	-
165	-	-	-	-	-	-	-	-22	-	-

3.2.1 CORRELATION ANALYSIS

The following cross-sections correlates the Self-Potential (mV) profiles, SP contours and 3-D SP plots, VES logs and 2-D ERT geo-electric sections to compare leachate contaminated areas along the survey lines (Figures 19 – 28):

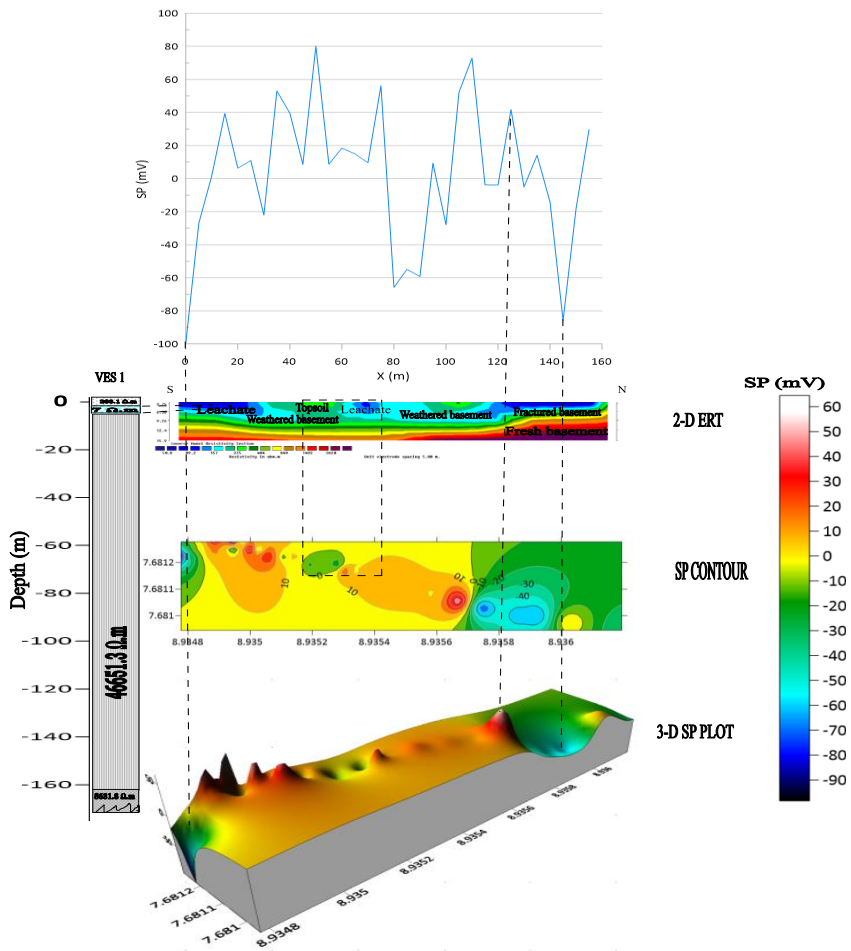


Figure 19: Cross-section correlating the 2-D ERT geo-electric section, VES transverse, Self-Potential in (mV) signal, SP contour and 3-D SP plot along profile 1

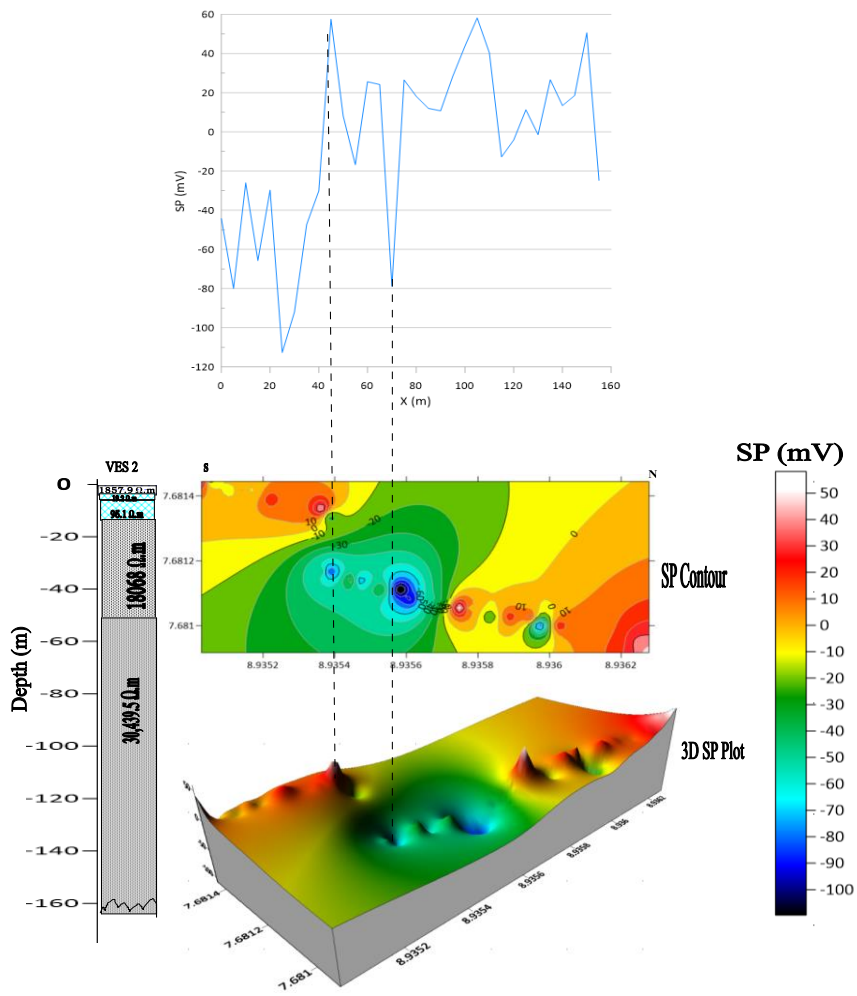


Figure 20: Cross-section correlating the VES transverse, Self-Potential in (mV) signal, SP contours and 3-D SP plot along Profile 2

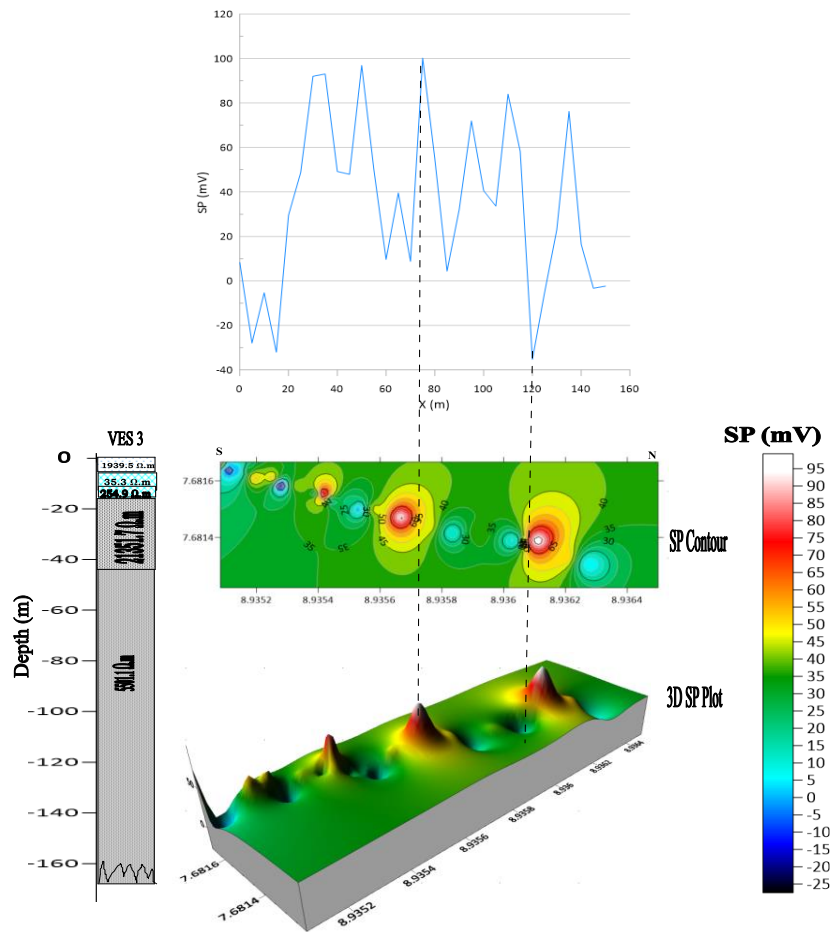


Figure 21: Cross-section correlating the VES transverse, Self-Potential in (mV) signal, SP contours and 3-D SP plot along Profile 3

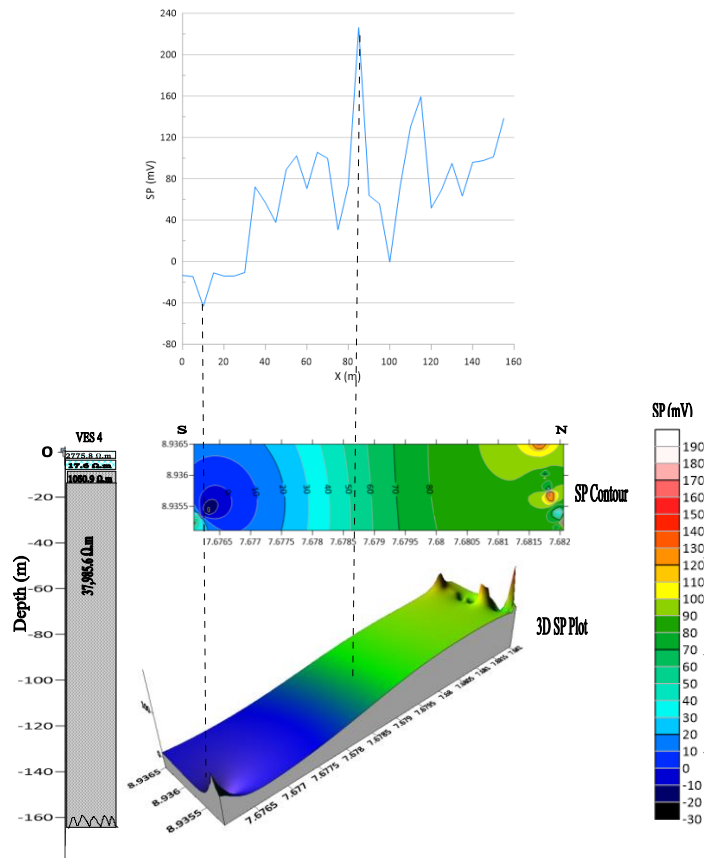


Figure 22: Cross-section correlating the VES transverse, Self-Potential in (mV) signal, SP contours and 3-D SP plot along Profile 4

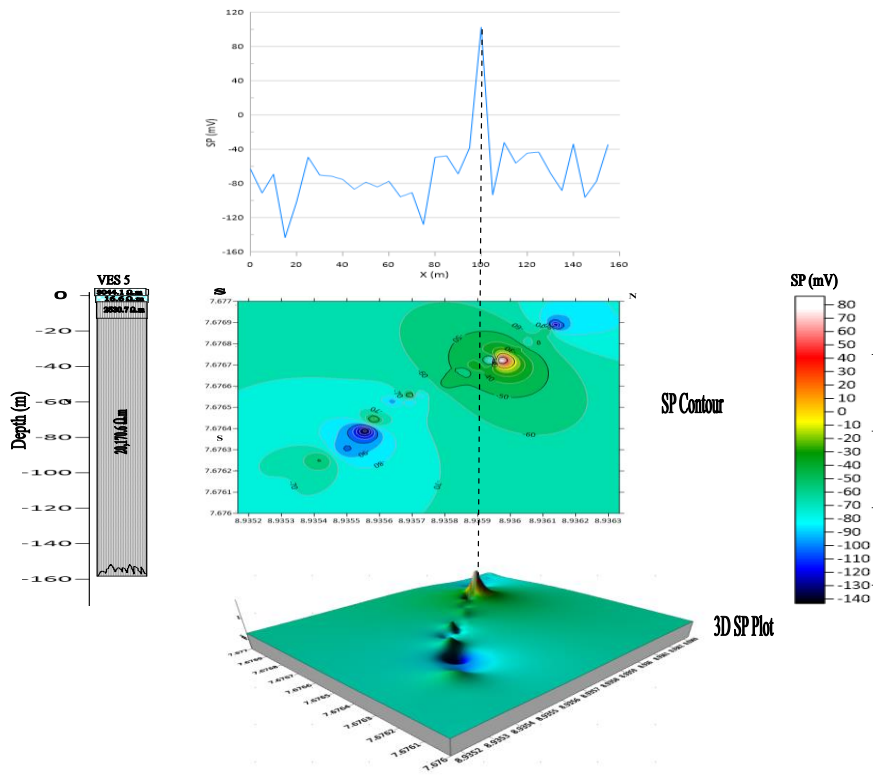
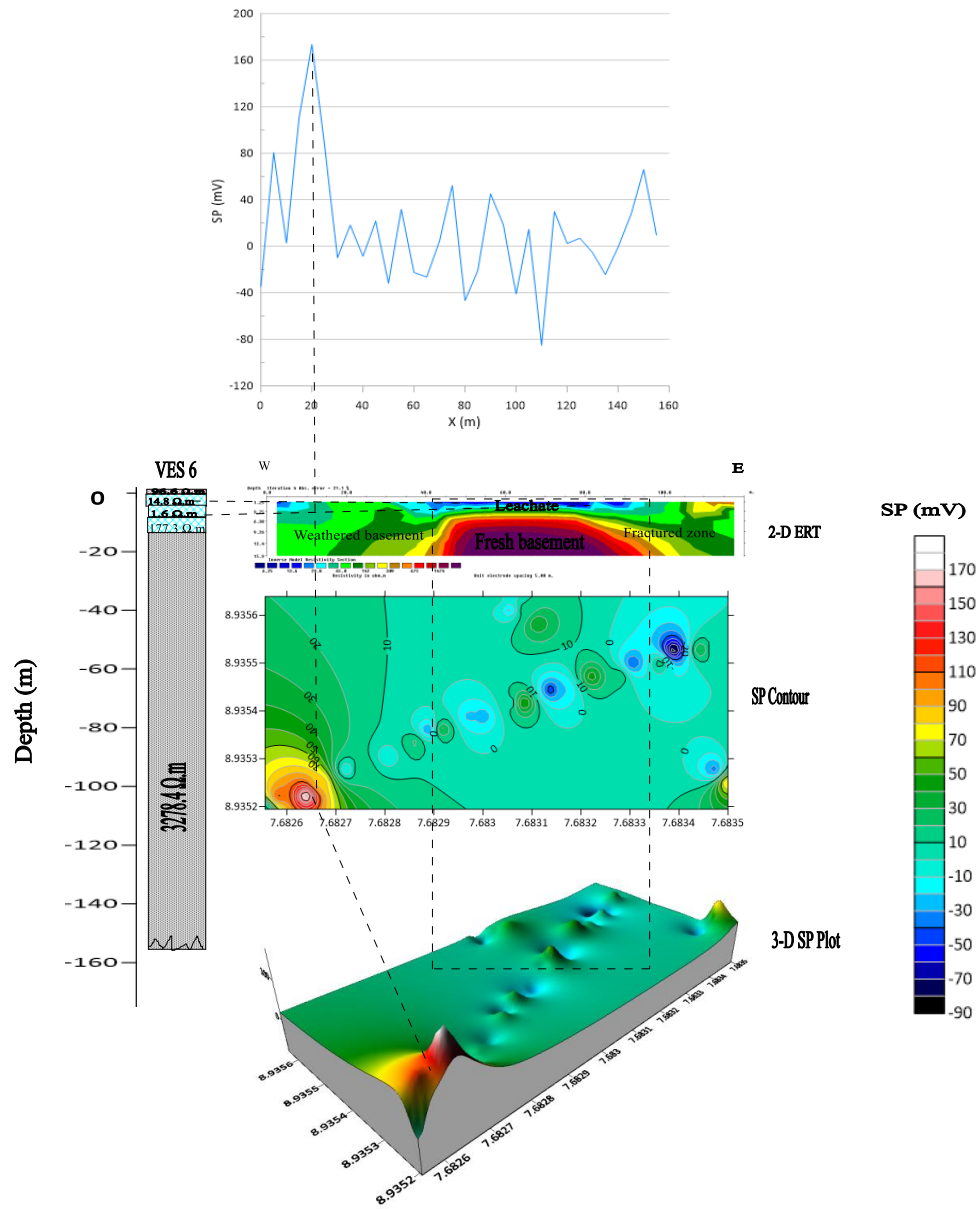


Figure 23: Cross-section correlating the VES transverse, Self-Potential in (mV) signal, SP contours and 3-D SP plot along Profile 5



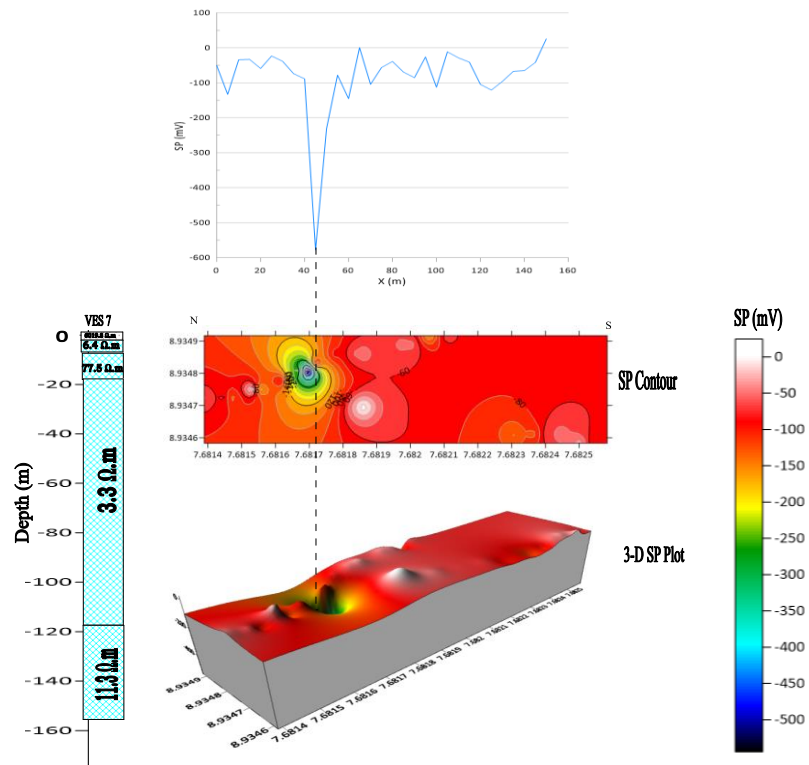


Figure 25: Cross-section correlating the VES transverse, Self-Potential in (mV) signal, SP contours and 3-D SP plot along Profile 7

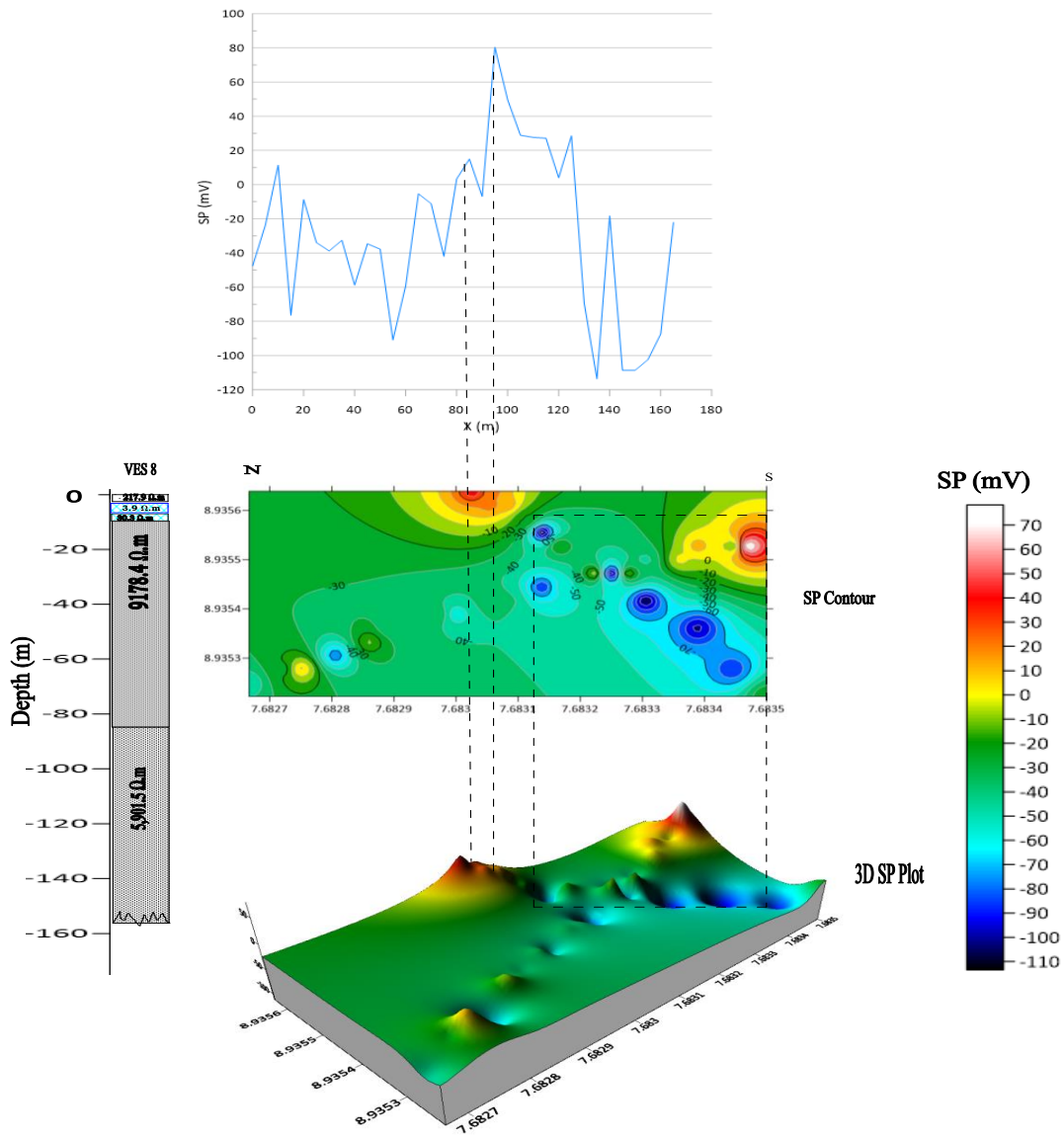


Figure 26: Cross-section correlating the VES transverse, Self-Potential in (mV) signal, SP contours and 3-D SP plot along Profile 8

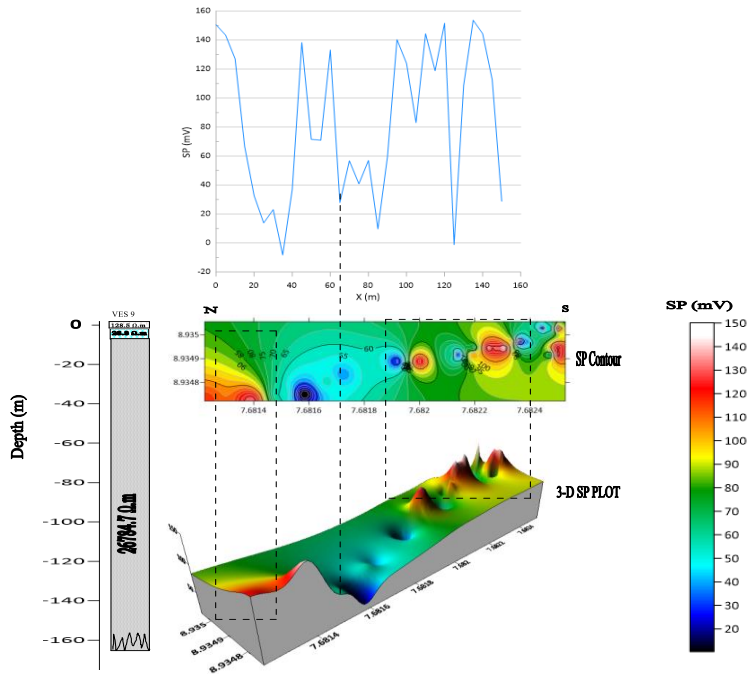


Figure 27: Cross-section correlating the VES transverse, Self-Potential in (mV) signal, SP contours and 3-D SP plot along Profile 9 (Goshen)

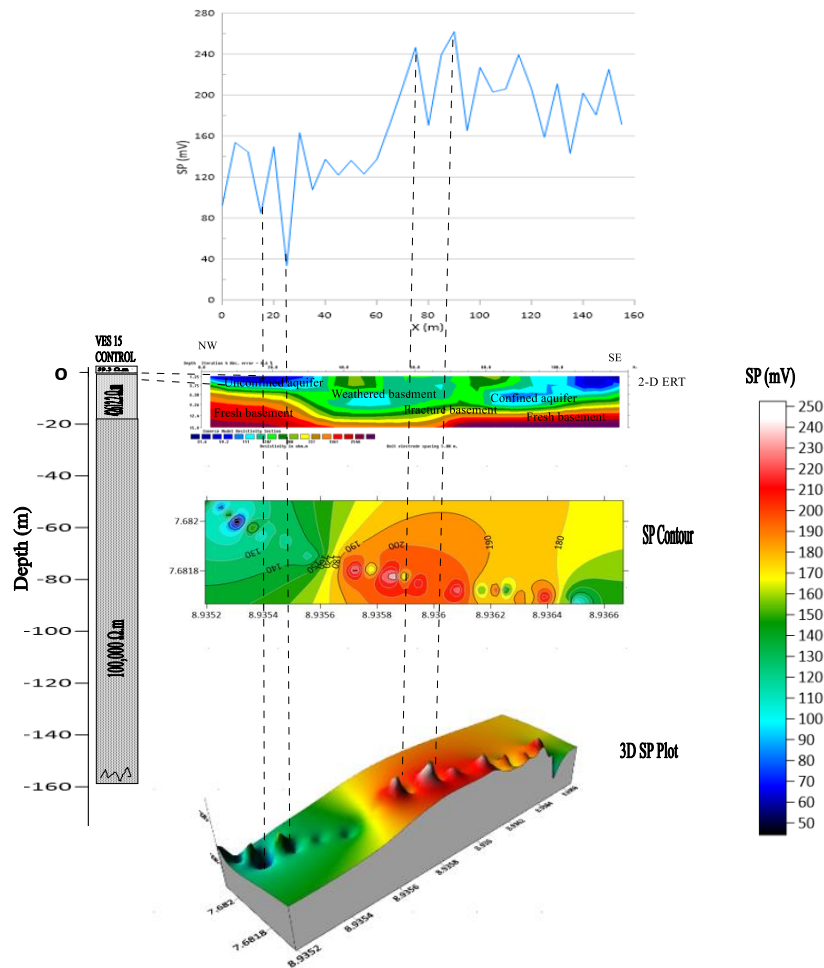


Figure 28: Cross-section correlating the VES transverse, Self-Potential in (mV) signal, SP contours and 3-D SP plot along the Goshen Control Centre

3.2.1 Discussion

3.2.2 Profile 1

The cross-section (Figure 19) correlates the 2-D ERT geo-electric section, SP profile, SP contours, 3-D SP plot, and VES Log, along profile 1. Starting from the southern flank in the 2-D ERT line are materials with low resistivity values ranging from (50.8 to 53 Ω .m, at depths \geq 6.38 m) between (0 to 20 m). This is suggestive of weathered layer infiltrated by leachate contaminants. To the northern flank, spanning between (50 to 90 m), are materials with similar resistivity values ranging from (49 to 51 Ω .m). This was also interpreted as sandy weathered/fractured zone hosting conductive materials. The dominant negative SP anomalies ranging from (-80 to -30 mV) situated between (0 to 10 m), and the SP anomalies ranging from (-90 to -40 mV) situated between (120 and 140 m) are attributed to differences in mobility and concentration of ions emanating from percolated organic and inorganic materials from the dumpsite. The materials with low resistivity values of (7 Ω .m, at depths \geq 2.2 m) along the VES log, suggests accumulation of leachate which correlates with the SP and 2-D ERT results.

3.2.1 Profile 2

The cross-section (Figure 20) correlates the SP (in mV) profile, the SP contours, the 3-D SP plot and the VES log for profile 2. Self-Potential profile shows variation of positive and negative SP values ranging from (-100 to 50 mV). The negative SP values peaked between (-90 to -30 mV) at the central point of the contour map situated between (60 to 100 m) interpreted as leachate contaminants flowing in the S–N direction. This correlated by presence of objects with low resistivity values of (19.2 Ω .m, at depth \geq 3.7 m) observed along the VES log interpreted as leachate infiltrated zone.

3.2.1 Profile 3

The cross-section (Figure 21) correlates the VES Log, 2-D SP contours, the 3-D SP plot and SP (in mV) signals for profile 3 running in the South – North direction. The self-potential profile in this cross-section shows variation of positive and negative SP values ranging from (-25 to 95 mV). However, the material with dominant negative SP values ranging from (-25 to -5 mV) which peaked between (0 to 20 m) and (110 and 120 m) is attributed to electrochemical reaction from groundwater flowing in the S-N direction. This result was correlated by materials with resistivity values of (35.3 Ω .m, at depth \geq 4.6 m) occurring along the VES transverse, suggestive of groundwater occurrence. The positive SP anomaly ranging from (40 to 95 mV) at points (55 and 75 m) along the profile is characteristic of quartz veins.

3.2.1 Profile 4

The cross-section (Figure 22) correlates the VES Log, 2-D SP contours, the 3-D SP plot and SP (in mV) signals for profile 4. It indicates variation of positive and negative SP values ranging from (-41 to 220 mV). From the southern flank, (0 to 40 m) are objects dominated by (-30 to -10 mV) negative SP values attributed to electro-kinetic processes occasioned by leachate plume from the dumpsite running in the North – South direction. This was correlated by VES log 4 indicating materials with the low resistivity values of (17.6 Ω .m, at depth \geq 3.6 m) observed beneath the topsoil along the profile.

3.2.1 Profile 5

The cross-section (Figure 23) correlates the SP (in mV) profile, VES Log, 2-D SP contours, the 3-D SP plot for profile 5. It shows the variation of positive and negative SP values ranging from (-140 to 90 mV). The undulating variation of the negative SP anomalies ranging from (-140 to -10 mV) peaked at points located between (15 to 20 m, 75 to 80 m and 130 to 145 m) and it is attributed to leachate infiltration flowing in the N-S direction, along the survey line. This was correlated by the VES log 5 showing materials with low resistivity values of (16.6 Ω .m, at depth \geq 5.5 m) along the VES transverse, suggestive of leachate infiltrated zone.

3.2.1 Profile 6

The cross-section (Figure 24) correlates the 2-D ERT, SP contours, 3-D SP plot and SP profile (in mV) and VES log for profile 6. The 2-D ERT line running in the W – E direction. From the southern flank in transverse 2, are materials with low resistivity values ranging from (5.8 to 6.5 Ω .m, at depths \geq 3.78 m) between (0 to 10 m). This is suggestive of areas infiltrated by leachate contaminants. To the northern flank, are materials with similar resistivity values ranging from (5.8 to 6.2 Ω .m) spanning between (40 to 140 m, depths \geq 3.78 m) interpreted as leachate plumes. The

VES log correlated these results with the materials of low resistivity values ranging from (1.6 and 14.8 Ω .m, at depths \geq 9.6 m) in the second and third layers interpreted as leachate infiltrated zone. These were further correlated by the dominant negative SP values ranging from (-90 to -10 mV) distributed along (40 to 140 m), suggestive of leachate infiltrated zone.

3.2.1 Profile 7

The cross-section (Figure 25) correlates the SP (in mV) profile, SP contours, the 3-D SP plot and the VES log for profile 7. The self-potential values for profile 7 shows dominant negative SP values ranging from (-550 to 0.2 mV) along the entire profile line spanning from (0 to 160 m) in N - S direction. The negative SP values peaked at (-560 mV) between (30 to 40 m) attributed to leachate infiltration into a fault/fractured layer. This was correlated by the VES log is characterized by materials beneath the topsoil; with low resistivity value of (6.4 Ω .m, at depth \geq 8.5 m). The second layer is characterized by a material with resistivity value of (77.5 Ω .m, at depths \geq 23.4 m) interpreted as weathered layer. Beyond this layer are materials with very low resistivity values ranging from (3.3 to 11.3 Ω .m, at depths \geq 123.4 m) suggestive of leachate infiltrated zone. This profile is interpreted as the most leachate impacted zone within the entire study area. It has been determined that groundwater resources in the area are likely contaminated due to the depth and extent of leachate migration into the subsurface.

3.2.1 Profile 8

The cross-section (Figure 26) correlates the VES Log, 2-D SP contours, the 3-D SP plot and SP (in mV) signals for profile 1-H running in the North – South direction. The self-potential profile shows variation of positive and negative SP anomalies ranging from (-110 to 80 mV) along profile 8. The negative SP values ranging from (-90 and -110 mV) peaked at points situated between (130 to 150 m), attributed to leachate infiltration zone flowing in the N - S direction, along the profile line. Also impacted are points located between (10 to 20 m) and (50 to 60 m) with corresponding SP values ranging from (-100 to -60 mV) suggestive of infiltrated leachate zone. These results were correlated by the VES 8 showing materials of low resistivity values ranging from (3.9 to 30.3 Ω .m, at depths \geq 5.7 m) interpreted as leachate infiltrated layers.

3.2.1 Profile 9

The cross-section (Figure 27) correlates the VES Log, 2-D SP contours, the 3-D SP plot and SP (in mV) signals for profile 9. The Self-Potential profile 9 shows an undulating section with negative SP anomalies ranging from (-5 to -10 mV) situated between (30 to 90 m) indicative of leachate infiltrated zone. The second layer within VES 9 reveals materials with low resistivity value of (28.3 Ω .m, at depths \geq 5.4 m) suggestive of weathered zone.

3.2.1 Profile 10 (Control Centre)

The cross-section (Figure 28) correlates the VES Log, 2-D ERT, SP contours, 3-D SP plot and SP profile (in mV) for the Control Centre. The SP profile at the control centre was dominated by positive SP values ranging from (50 to 250 mV) along the entire profile. This established the absence of leachate infiltration into the subsurface. The materials with highest resistivity values ranging from (31.3 to 59.2 Ω .m) recorded along the 2-D ERT section established that the control centre is devoid of leachate contaminants. The VES 10 correlated the 2-D ERT results showing

materials with high resistivity values ranging from (59.3 to 100,000 Ω .m, at depths ≥ 160 m), which established that the control centre is leachate free.

3.3 Interpretation of Very Low Frequency Electromagnetic (VLF-EM) results

The results for the ten (10) VLF-EM Transverses established on the southern part of the dumpsite (1 - 6); (7 to 9) on the northern part, and (10) at the control centre, indicating the Fraser filtered, measured VLF and K-H pseudo cross-sections are shown in Figures 29 to 38:

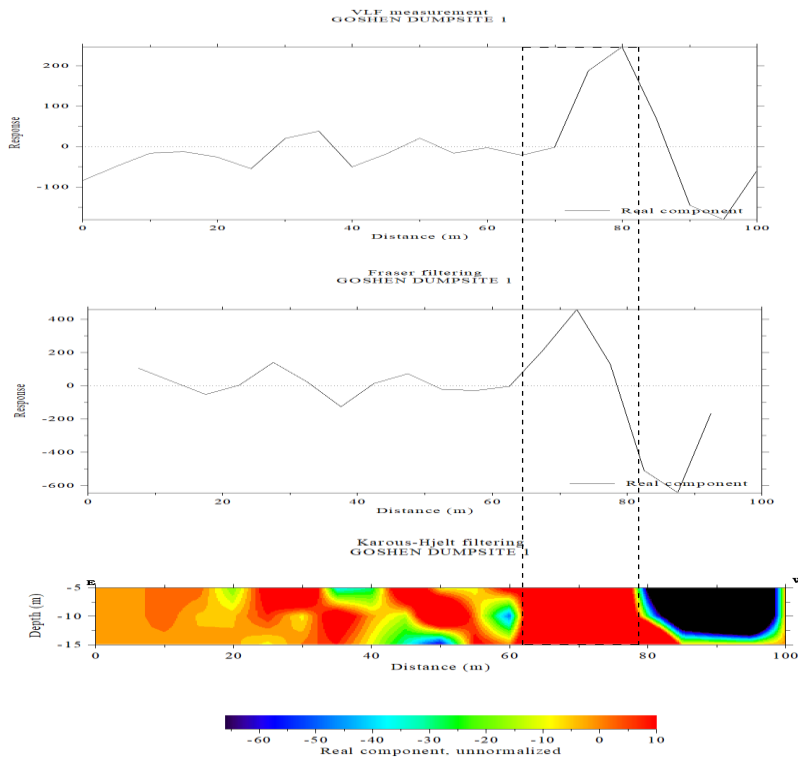


Figure 29: Cross-section of Fraser Filtered, measured VLF and K-H pseudo section along Transverse 1

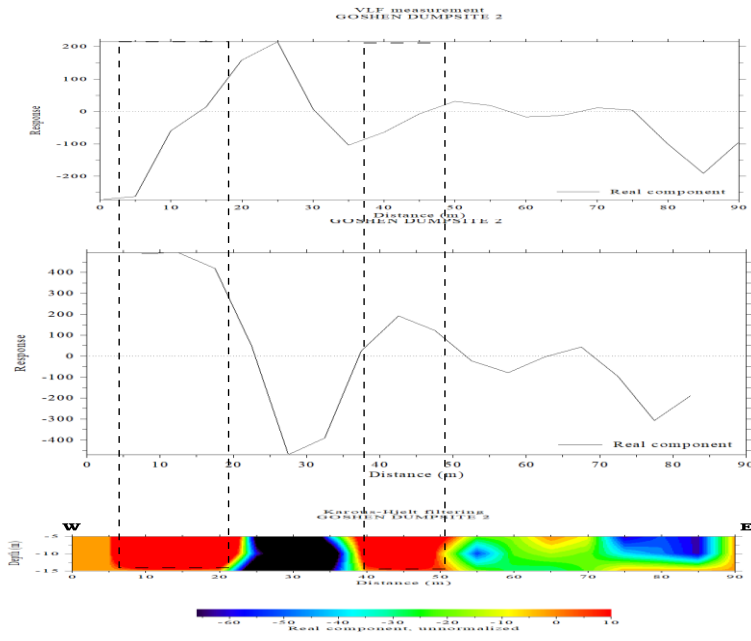


Figure 30: Cross-section of Fraser Filtered, measured VLF and K-H pseudo section along Transverse 2

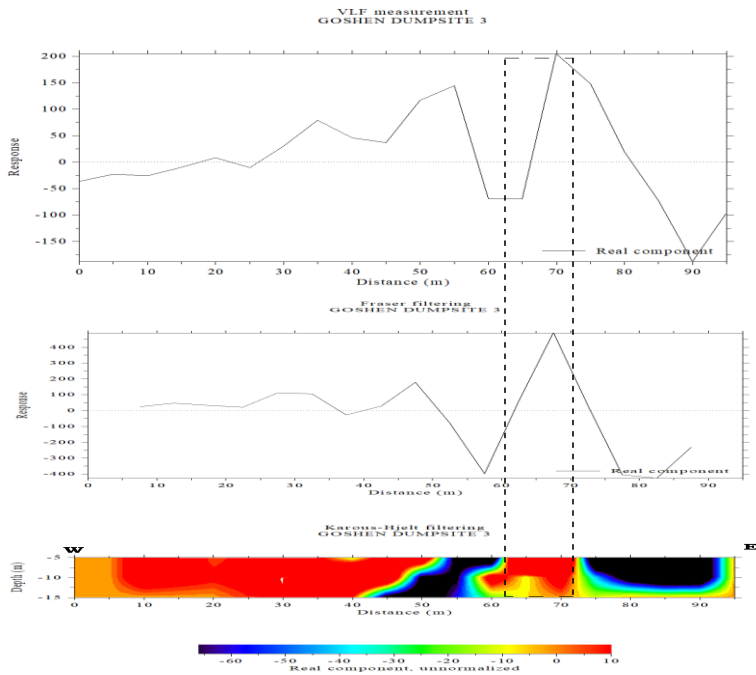


Figure 31: Cross-section of Fraser Filtered, measured VLF and K-H pseudo section along Transverse 3

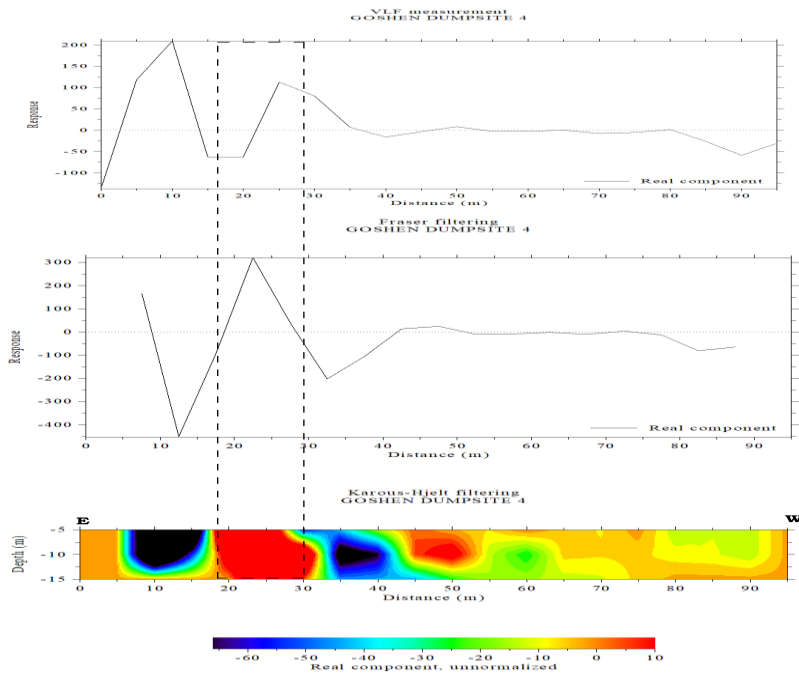


Figure 32: Cross-section of Fraser Filtered, measured VLF and K-H pseudo section along Transverse 4

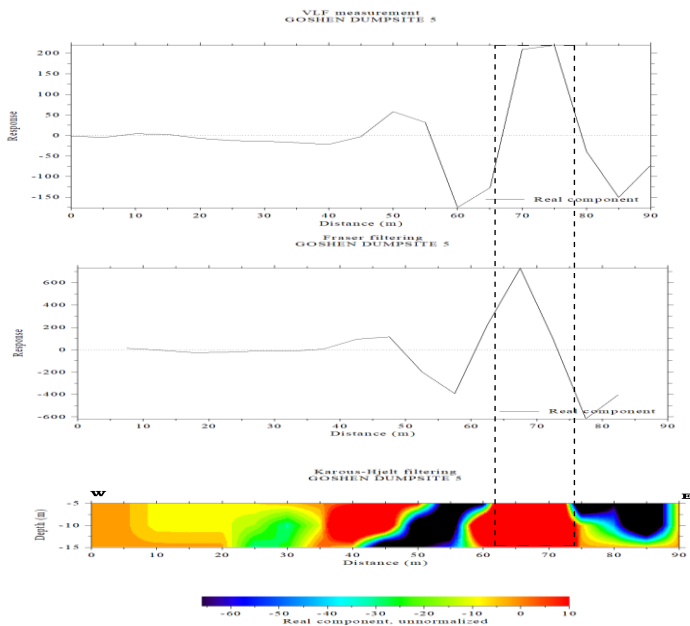


Figure 33: Cross-section of Fraser Filtered, measured VLF and K-H pseudo section along Transverse 5

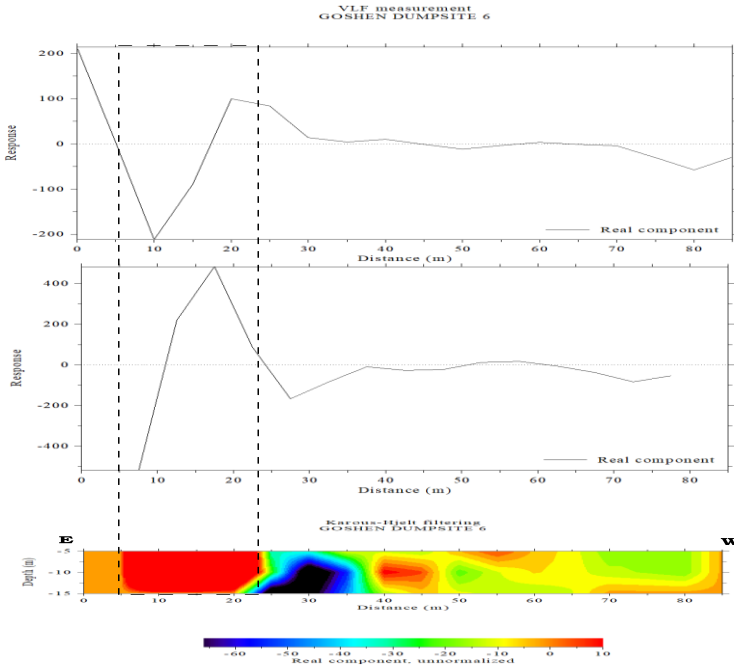


Figure 34: Cross-section of Fraser Filtered, measured VLF and K-H pseudo section along Transverse 6

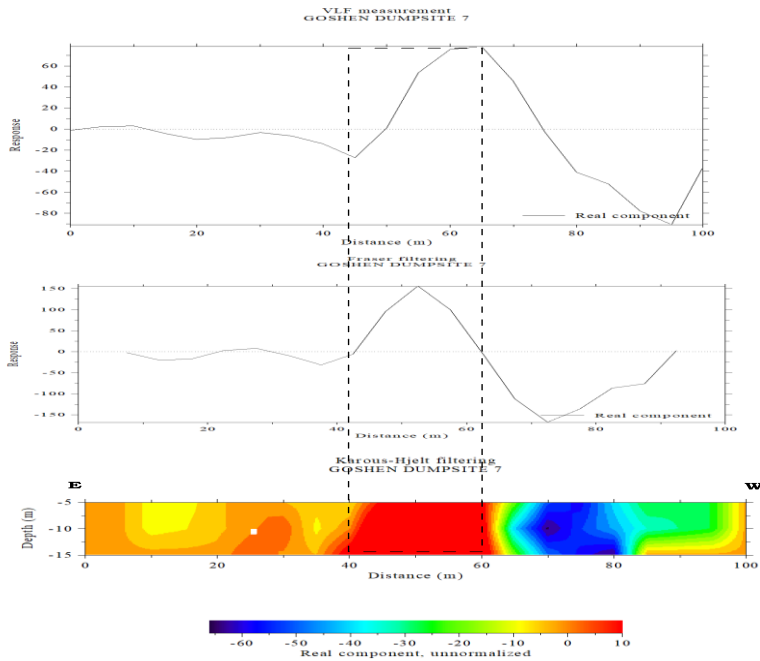


Figure 35: Cross-section of Fraser Filtered, measured VLF and K-H pseudo section along Transverse 7

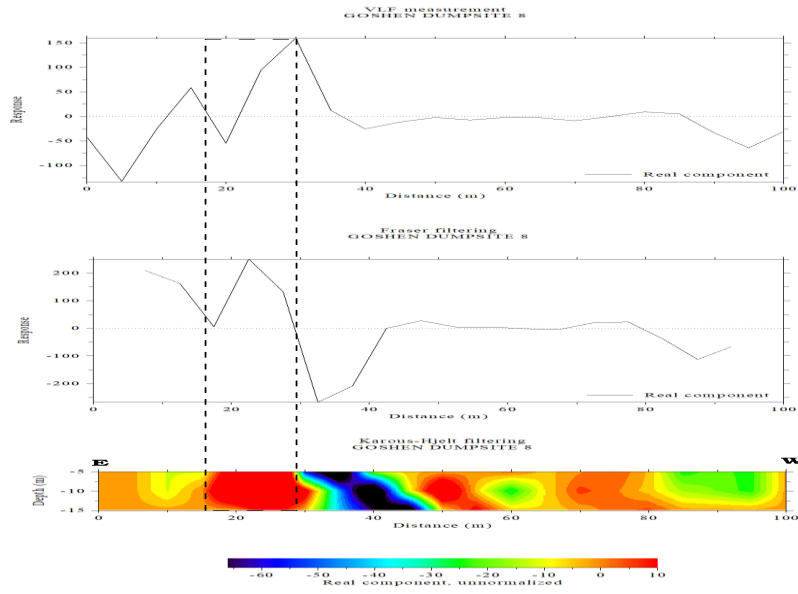


Figure 36: Cross-section of Fraser Filtered, measured VLF and K-H pseudo section along Transverse 8

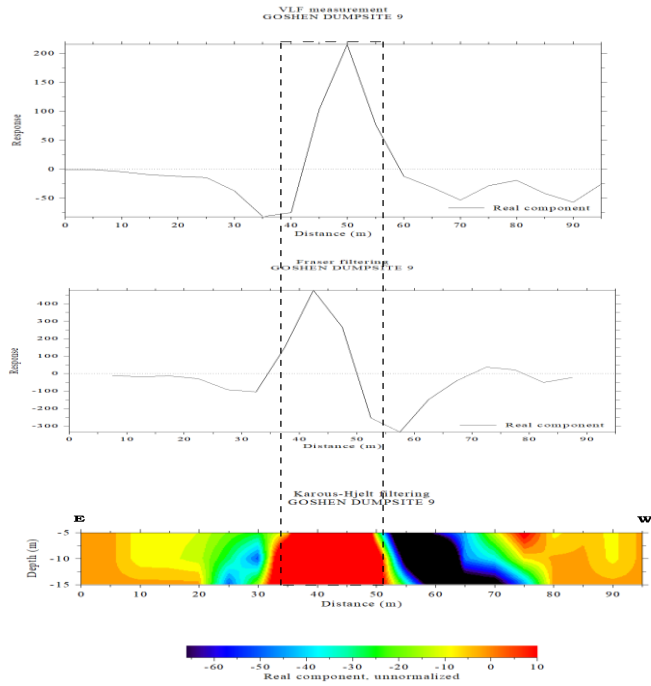


Figure 37: Cross-section of Fraser Filtered, measured VLF and K-H pseudo section along Transverse 9

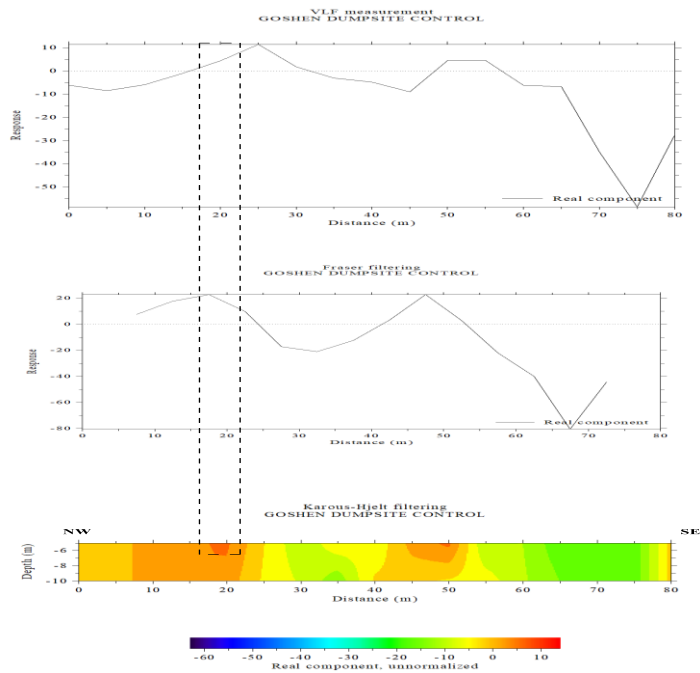


Figure 38: Cross-section of Fraser Filtered, measured VLF and K-H pseudo section along Transverse 10 (Control Centre)

3.3.1 Discussion

3.3.2 Transverse 1

The prominent high positive anomaly ranging from (5 to 10%) between (32 to 51 m, at depths ≥ 12 m) situated along Transverse 1 in the E – W direction, suggests the lateral and vertical spread of leachate from the dumpsite into the subsurface. The waste must have generated electrical conducting paths under the subsurface. Between (80 to 100 m, at depths ≥ 15 m) is a black material with high negative anomaly ranging from (-50 to -60 %). This is suggestive of mineralized concrete iron sandstone. At distances between (10 to 20 m, 38 to 41 m, and 41 to 50 m, depths ≥ 14 m) are greenish patches suggestive of rock intrusions. The anomalous conductive zones are suspected to be lineament structures while the resistive features are presumed to be lateritic/hardpan/basement formation.

3.3.3 Transverse 2

The high positive anomaly ranging from (5 to 10%) along (8 to 20 m, and 40 to 50 m depths ≥ 15 m) along Transverse 2 in the W – E direction is interpreted as the migration of leachate contaminant into the subsurface. Between (20 to 40 m, at depths ≥ 15 m) is a black material with negative anomaly ranging from (-50 to -60 %), suggestive of pegmatites veins which outcrops the area. At points between (50 to 90 m, at depths ≥ 14 m), are intercalations of greenish, bluish and

lemon coloured materials suggestive of rock intrusions. The anomalous conductive zones are suspected to be lineament structures while the resistive features are presumed to be weathered bedrock.

3.3.4 Transverse 3

The anomaly (highly positive) ranging from (5 to 10%) along (10 to 40 m, and 60 to 70 m, at depths ≥ 15 m) of Transverse 3 in the W – E direction is suggestive of leachate infiltration. Situated between (40 to 60 m and 70 to 100 m, at depths ≥ 15 m) are black materials with high negative anomaly ranging from (-50 to -60 %). The anomalous conductive zones are suggestive of lineament structures.

3.3.5 Transverse 4

The prominent high positive anomaly ranging from (5 to 10%) along (20 to 30 m and 42 to 52 m, at depths ≥ 14 m) extending to depths of (5 to 14 m, at depths ≥ 15 m) along the survey line is suggestive of infiltration of leachate into the subsurface flowing in the E – W direction. Black materials with high negative anomaly ranging from (-50 to -60 %) located between (5 to 20 m and 30 to 40 m, at depths ≥ 15 m) are suggestive of fractured zone hosting pegmatite veins which outcrops the area. The materials consisting of intercalations of lemon, yellowish and orange coloured patches situated between (55 to 100 m) are suggestive of various rock materials. The anomalous conductive zones are suspected to be lineament structures while the resistive features are presumed to be hardpan or basement formation.

3.3.6 Transverse 5

The prominent materials with high positive anomaly ranging from (5 to 10%) situated between (60 to 70 m and 30 to 40 m, at depths ≥ 14.5 m) extending to depths of (5 to 15 m depths ≥ 13 m) along the survey line in the W – E direction is suggestive of lateral and vertical spread of leachate into the subsurface. The black materials with high negative anomaly ranging from (-50 to -60 %) situated between (40 to 60 m and 70 to 90 m, at depths ≥ 15 m) are suggestive of fractured zone hosting pegmatite veins which outcrops the area, while the intercalations of materials with lemon, yellowish and orange coloured patches located between (0 to 30 m, at depths ≥ 14.5 m) are suggestive of hardpan.

3.3.7 Transverse 6

The materials with high positive anomaly ranging from (5 to 10%) along (5 to 21 m, depths ≥ 15 m) extending to depths of (5 to 15 m, at depths ≥ 14 m) along the survey line is interpreted as leachate contaminated zone flowing in the E – W direction. The black materials negative anomaly ranging from (-50 to -60 %) between (21 to 35 m) are suggestive are of fractured layer hosting mineralized rocks. The materials with intercalations of lemon, yellowish and orange coloured patches, situated between (40 to 100 m, at depths ≥ 14.8 m) are suggestive of various rock materials.

3.3.8 Transverse 7

The materials with high positive anomaly ranging from (5 to 10%) situated along (20 to 40 m and 40 to 60 m, at depths ≥ 15 m) extending to depths of (5 to 15 m, at depths ≥ 14.8 m) in the E – W direction are suggestive of leachate infiltration. The intercalations of lemon, yellowish and orange

coloured patches, located between (60 to 100 m, at depths ≥ 14.7 m) are suggestive of various rock materials.

3.3.9 Transverse 8

The materials with positive anomaly ranging from (5 to 10%) situated along (10 to 28 m and 45 to 60 m, at depths ≥ 15 m) along the survey line in the E – W direction is suggestive of lateral and vertical spread of leachate from the dumpsite into the subsurface. The greenish circular object situated between (55 to 61 m) is interpreted as hematite intrusion. On the right flank spanning from (60 to 100 m, at depths ≥ 14 m) is another greenish material suggestive of a rock. Between (5 to 15 m, at depths ≥ 14 m) is a yellowish material interpreted as dolomite.

3.3.10 Transverse 9

The materials in the E-W direction with prominent high current density anomaly ranging from (5 to 10%) along (30 to 50 m, at depths ≥ 15 m) along the survey line is suggestive of leachate infiltrated zone. Between (51 to 80 m) are black materials with high negative anomaly ranging from (-50 to -60 %) suggestive of fractured zone hosting mineralized rocks. Between (0 to 10 m and 29 to 30 m, at depths ≥ 15 m) are patches of yellowish and orange materials, suggestive of fractured rocks. Between (80 to 100 m, at depths ≥ 14.1 m) are yellowish and orange coloured materials suggestive of pegmatite intrusive rocks.

3.3.11 Transverse 10 (Control Centre)

The results at the control centre situated 500 m away from the dumpsite revealed that they were materials with lesser current density anomaly ranging from (5 to 6 %) situated along (10 to 20 m, at depths ≥ 15 m) trending in the NW – SE direction. The materials with green, lemon and yellow patches were inferred as weathered/fractured materials hosting groundwater resources. Comparatively, the low positive anomaly recorded at control centre established that the area was not impacted by leachate contamination.

4.1 Conclusion

The study demonstrated the effectiveness of combining VES, 2-D ERT, SP, and VLF-EM geophysical methods to investigate aquifer vulnerability near a major dumpsite in Goshen City, Nasarawa State, Nigeria. The methods identified low resistivity materials ranging from (1.6 to 35.3 Ω .m, at an average depths ≥ 15.8 m, along VES (1, 2, 3, 4, 5, 6, 7, 8, 9, 10, 12 and 14) as leachate infiltrated zones. Negative SP anomalies ranging from (-578 to -2.4 mV) were attributed to electrokinetic process emanating from percolated organic and inorganic materials from the dumpsite, while materials with high positive VLF current-density ranging from (5 to 10 %, depths ≥ 15 m), were interpreted as electrical conducting paths generated by leachate. The percentage (80%) of the combined VES points indicating weak to poor aquifer protective capacity, suggests that the study area is unsuitable for a dumpsite establishment. Continuous monitoring and the installation of geosynthetic clay liners at the base of the dumpsite to safeguard groundwater resources from leachate infiltration are therefore recommended.

Disclaimer (Artificial intelligence)

Author(s) hereby declare that NO generative AI technologies such as Large Language Models (ChatGPT, COPILOT, etc.) and text-to-image generators have been used during the writing or editing of this manuscript.

References

1. Abdel-Shafy, H. I., Ibrahim, A. M., Al-Sulaiman, A. M., & Okasha, R. A. (2024). Landfill leachate: Sources, nature, organic composition, and treatment: An environmental overview. *Ain Shams Engineering Journal*, 15(1), 102293. DOI: <https://doi.org/10.1016/j.asej.2023.102293>
2. Adeniji, A. A., Ajani, O. O., Adagunodo, T. A., & Kolawole, T. (2024). Investigation of leachate infiltration on groundwater using georesistivity and natural electric field method around Ojoou-Olayanju's dumpsite, Ada, southwestern Nigeria. *Nigerian Journal of Technology*, 43(1), 159-171. DOI: <https://doi.org/10.4314/njt.v43i1.18>
3. Bashir, M. Z. (2018). Geology of The Area Around Kurafe Hausawa, Part of Keffi Sheet 208 nw. 61.
4. Dada, S. S. (2006). Proterozoic evolution of Nigeria. *The basement complex of Nigeria and its mineral resources (A Tribute to Prof. MAO Rahaman)*. Akin Jinad and Co. Ibadan, 29-44.
5. Dauda, G., and Ali, A. M. (2024). Delineating leachate-groundwater interaction at Gyadi-Gyadi dumpsite, Kano, using natural electromagnetic (EM) field detector and Vertical Electrical Sounding (VES). *Geosystems and Geoenvironment*, 3(4), 100303. DOI: <https://doi.org/10.1016/j.geogeo.2024.100303>
6. Google Earth Engine. A Planetary-Scale Platform for Earth Science & Data Analysis. Available online: <https://earthengine.google.com/> (accessed on 20 November 2024).
7. Igwegbe, C. A., López-Maldonado, E. A., Landázuri, A. C., Ovuoraye, P. E., Ogbu, A. I., Vela-García, N., & Białowiec, A. (2024). Sustainable municipal landfill leachate management: Current practices, challenges, and future directions. *Desalination and Water Treatment*, 100709. DOI: <https://doi.org/10.1016/j.dwt.2024.100709>
8. NGS (Nigeria Geological Survey Agency) (2011). Geological map of Abuja. Published by the Authority of the Federal Republic of Nigeria.
9. Odoh, B. I., Korie, J. I., Arukwe-Moses, C. P., Ahaneku, C. V., Azike, M. C., Muogbo, C. D., & Chibuzor, S. N. (2024). Assessing the Impact of Leachate Infiltration from Dumpsites into the Groundwater System of Agu-Awka and Environs, Southeastern Nigeria. *Journal of Geography, Environment and Earth Science International*, 28(8), 141-160. DOI: <https://doi.org/10.9734/jgeesi/2024/v28i8804>
10. Onicha, A. D., Onwe, J. C., Ngwuta, N. O., Oguma, S., & Jahanger, A. (2024). Attaining sustainable development in Nigeria: the role of solid waste, urbanization and pollution in reducing under-five mortality. *Discover Sustainability*, 5(1), 357. DOI: <https://doi.org/10.1007/s43621-024-00570-2>

11. Oversby, V. M. (1975). Lead isotopic study of aplites from the Precambrian basement rocks near Ibadan, southwestern Nigeria. *Earth and Planetary Science Letters*, 27(2), 177-180.
12. Peter, A., Mallam, A., & Abdulsalam, N. N. (2016). Geo-electrical investigation of subsurface water resources in Kutunku, Gwagwalada Area Council, Abuja, Nigeria. *IOSR J. Appl. Physics*, 8(5), 9-18.
13. Sanuade, O. A., Arowoogun, K. I., & Amosun, J. O. (2022). A review on the use of geoelectrical methods for characterization and monitoring of contaminant plumes. *ActaGeophysica*, 70(5), 2099-2117. DOI: <https://doi.org/10.1007/s11600-022-00858-9>
14. Tanko, I. Y., Adam, M., and Dambring, P. D. (2015). Field features and mode of emplacement of pegmatites of Keffi area, north central Nigeria. *International Journal of Scientific & Technology Research*, 4, 214-229.
15. Udosen, N. I., Ekanem, A. M., & George, N. J. (2024). Geophysical exploration to assess leachate percolation and aquifer protectivity within hydrogeological units at a major open dump in Eket, Nigeria. *Results in Earth Sciences*, 2, 100022. DOI: <https://doi.org/10.1016/j.rines.2024.100022>